Travelling wave mathematical analysis and efficient numerical resolution for a realistic model of solid propellant combustion

Laurent François, Joel Dupays, Dmitry Davidenko, Marc Massot

DOI: 10.13009/EUCASS2019-624

DOI: ADD DOINUMBER HERE

Travelling wave mathematical analysis and efficient numerical resolution for a realistic model of solid propellant combustion

Laurent François[1,2]*, Joël Dupays*[1]*, Dmitry Davidenko*[1]*, Marc Massot*[2]*,*
[1] *ONERA, DMPE, 6 Chemin de la Vauve aux Granges, 91120 Palaiseau, France*
[2] *CMAP, CNRS, Ecole polytechnique, Institut Polytechnique de Paris,*
Route de Saclay, 91128 Palaiseau Cedex, France
{laurent.francois, joel.dupays, dmitry.davidenko}@onera.fr · marc.massot@polytechnique.edu

Abstract

We investigate a model of solid propellant combustion involving surface pyrolysis coupled to finite activation energy gas phase combustion at unit Lewis number. Existence and uniqueness of a travelling wave solution are established by extending dynamical system tools classically used for premixed flames, dealing with the additional difficulty arising from the surface regression and pyrolysis. An efficient shooting method allows to solve the problem in phase space without resorting to space discretization nor fixed-point Newton iterations. The results are compared to solutions from a CFD code developed at ONERA, assessing the efficiency and potential of the method.

1. Introduction

Solid propellant combustion is a key element in rocket propulsion and has been extensively studied since the 1950s including at ONERA [1, 2, 3, 4]. This particular problem involves a solid phase and a gas phase, separated by the interface (surface of the solid). The solid is heated up by thermal conduction and radiation from the gas phase. At its surface, the solid propellant is decomposed through a pyrolysis process, and the resulting pyrolysis products are gasified and injected in the gas phase. Both these phenomena will be gathered under the name "pyrolysis" for simplicity. The interface regresses and the injected species react and form a flame, which heats back the solid and allows for a sustained combustion. It is essential to understand the physics of this phenomenon to allow for clever combustion chamber designs and efficient solid rocket motors. A key element is the regression speed of the propellant's surface, and its variations depending on the combustion chamber conditions.

Many models with variable level of detail have been developed, with essentially two levels of description. On the one side, there exists analytical models, which directly give a formula for the steady regression speed and allow a qualitative description and global understanding of the physics at the cost of some restrictive assumptions. On the other side, one can find detailed models, that require high-fidelity numerical resolution with spatial and temporal discretizations (CFD), giving a very detailed representation of the physics, both for quasi-steady and unsteady evolutions. The main analytical models in steady regime are the Denison-Baum-Williams (DBW) model [5], the Beckstead-Derr-Price (BDP) model [6] and the Ward-Son-Brewster (WSB) model [7]. They mainly give the regression speed and the surface temperature, using a one-dimensional approach. They usually assume the pyrolysis is concentrated at its surface and the gas phase only contains two species: one reactant resulting from the pyrolysis, and one product. There is only one global reaction which transforms the reactant into the product. The DBW and BDP models assume that the activation energy E_a of the gas phase reaction is very high. This allows the splitting of the gas phase into two separate zones: the convection-diffusion zone and the reaction-diffusion zone, starting at the flame stand-off distance x_f (model-specific). The equations can be solved in each zone separately and linked at the interface between the two, yielding an analytical expression for the burning mass flow rate $\dot{m}$. On the opposite, the WSB model assumes that E_a is zero, which often leads to better agreement with experimental results. Assuming a unitary Lewis number, several equations can be derived, which require simple fixed-point iterations to determine the regression speed. All these models give analytical relations between the propellant physical characteristics and the physical state of the propellant and gas flow (surface temperature, regression speed). They give a global understanding of the phenomenon. In all these models, the equations

DOI: 10.13009/EUCASS2019-624

describing the physics of both phases can only be solved for a unique value of the regression speed c, called the "eigenvalue" of the problem.

On the other end of the spectrum, numerical methods solving a comprehensive set of equations, e.g. [8], use much less restrictive assumptions, but they are computationally expensive and may encounter difficulties converging, potentially requiring transient evolutions. Their results are case-specific and do not allow for generic relations to be established between the different parameters.

It would therefore be interesting to have an easy-to-use and yet precise analytical or semi-analytical model (i.e. requiring numerical iterations), that would not require as many assumptions as the existing analytical models and thus remain closer to the physics. Such a model does already exist for travelling combustion wave in laminar premixed flames and has been studied for quite some time, for example in [9]. This model is based on a phase-plane representation of a simplified combustion problem with unitary Lewis number, two species and a single reaction. The combustion wave speed is shown to be a key parameter for which only one value allows the simplified problem to be solved. This value can be determined numerically through a shooting method, for any value of the activation energy of the gas phase reaction.

In this paper, we investigate a specific model of solid propellant combustion. It involves pyrolysis in an infinitely thin zone at the interface coupled to solid regression and homogeneous gas phase combustion described by one global reaction with finite activation energy at unit Lewis number. The model is derived from a detailed system of equations that describes the evolution of the temperature of the solid propellant, the evolution of the gas phase, and the pyrolysis of the propellant. The model takes into account thermal expansion and density changes in the gas phase. We study the travelling wave solution of this system of equation, that is we look for a temperature profile and a wave velocity c, the so-called eigenvalue. In the case of a solid propellant, Verri [10] presented a demonstration of the uniqueness of the solution and its stability using a different approach, without modelling the gas phase, but only considering the gas heat feedback as a function of the regression speed with specific mathematical properties. However, in solid propellant configuration, the separation of the problem into a gas phase and a solid phase, with a non-trivial coupling condition at the interface on fluxes, introduces additional difficulties, such as a temperature gradient jump depending on the eigenvalue. These difficulties are overcome through a detailed dynamical system study of such an heteroclinic orbit in phase space, allowing us to prove the existence and uniqueness of both the self-similar profile and eigenvalue. The approach is similar to the one used by Zeldovich et al. [9] in the study of laminar flames. Interpretation of the phase space also allows to better understand the role of the interface and the influence of the different parameters. A numerical shooting method is then developed to iteratively find the speed of the wave and ultimately its profile with arbitrary precision. To the best of our knowledge, no such study has yet been presented. We also propose to assess the efficiency and potential of the method by first verifying the proposed numerical strategy in comparison to a CFD code developed at ONERA with the same level of modelling and then follow up with a parametric study of the influence of the activation energy of the chemical reaction in the gaseous phase. Eventually, the improvement of our approach compared to the analytical model is investigated as well as the influence of assumptions such as the unitary Lewis number.

The paper is organized as follows: In section 2, we first introduce the generic equations describing the gas flow, the solid phase and the coupling conditions. Adding a series of assumptions, we gradually simplify the system, while still retaining the most important physical aspects, and introduce a travelling wave solution and derive the equations that describe the wave profile. The impact of the wave speed c is explained. We derive some general relations to obtain characteristic values for a non-dimensionalization of the problem. In section 3, extending Zeldovich's approach for laminar flames, we prove the existence and uniqueness of the self similar temperature profile and wave speed by a dynamical system approach and focus on how to handle the specific solid-gas interface flux condition. A physical interpretation of the result is given. Section 4 is devoted to the presentation of the various algorithms used in the numerical resolution based on a shooting method, and the comparison for various levels of modelling assumptions with a CFD code developed at ONERA. A conclusion on the efficiency and the potential of the approach is given in section 5.

2. General modelling, proper set of simplifications and travelling wave formalism

In this section we start by presenting the general assumptions usually made for the development of advanced models for high-fidelity simulations. Introducing additional assumptions that are not too restrictive, we derive another set of equations that is simple enough to envision an analytical study of travelling wave solutions. Although this system is much simpler, it is expected to give a realistic picture of the combustion of a solid propellant.

DOI: 10.13009/EUCASS2019-624

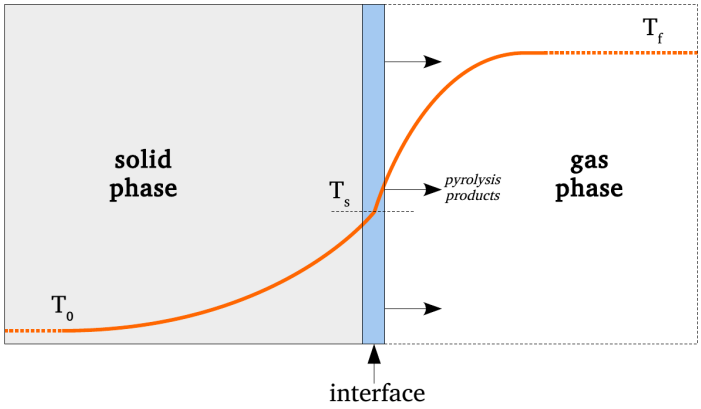

Figure 1: 1D model of a solid propellant burning

2.1 Derivation of the model, related assumptions and travelling wave formulation

Composition and temperature variations in the solid phase decomposition zone and in the gas flame structure are often important in the direction normal to the burning propellant surface, so that it is common to adopt a one-dimensional approach, which greatly simplifies the mathematical developments. The phenomenon is studied in the Galilean reference frame $\mathscr{R}_G$ and a schematic representation is provided in Figure 1. The solid phase (the propellant) is semi-infinite and is located between $-\infty$ and $x = \sigma(t)$ the position of the interface between the solid and gas phases. The gas phase is also semi-infinite and is located between $x = \sigma(t)$ and $+\infty$. The instantaneous regression speed is $c(t) = d_t\sigma(t)$. Most of the solid propellant numerical models assume the following:

H 1. *The solid phase is inert, incompressible and inelastic. No species diffusion takes place in the solid. Far from the burning surface, the solid phase is at its initial temperature, $T(-\infty) = T_0$. All gradients vanish at $x = -\infty$.*

H 2. *The gas phase is constituted of a mixture of reacting ideal gases in the low-Mach number limit and the pressure P does not vary with time.*

H 3. *No species or heat accumulation takes place at the interface. The temperature is continuous across the interface and its value is denoted $T_s(t)$. The gasification process is controlled by a pyrolysis reaction concentrated at the interface. The mass flow rate of gaseous species expelled by the solid phase through the pyrolysis reaction is given by a pyrolysis law of the form:*

$$\dot{m} = A_p \exp\left(-\frac{T_{ap}}{T_s}\right) \tag{1}$$

Some further assumption is proposed on the pyrolysis law. This modification has no impact on the physics. It is very similar to the cold boundary difficulty resolution [11] and will allow for a proper theoretical analysis.

H 4. *In fact, the propellant will not be consumed at $T_s = T_0$, T_0 being in all realistic cases close to the ambient temperature. That behaviour is not depicted exactly by the pyrolysis law* (1)*. Therefore we introduce a slightly modified pyrolysis law that contains a cut-off so that $\dot{m}$ smoothly goes to 0 as T_s approaches T_0:*

$$\dot{m} = A_p \exp\left(-\frac{T_{ap}}{T_s}\right) \phi(T_s - T_0) \tag{2}$$

with ϕ a C^∞ function, such that $\phi(y) = 0$ for $y \leq 0$ and $\phi(y)$ quickly reaches a value of 1 as y becomes greater than 0. The function ϕ can typically be a sigmoid function.

This simplified type of pyrolysis law is frequently used for stationary as well as transient studies of solid propellant combustion, although it ignores some important effects which only appears in more comprehensive zeroth-order pyrolysis relations, deduced for instance from activation energy asymptotics [12]. The pre-exponential factor may contain a dependence in pressure (typically P^n). Adding another dependence on T_s in the form of T_s^β with $\beta > 0$ is also possible, and would not affect the results presented further on. Note that all the conclusions made in this paper remain valid for any other pyrolysis law $\dot{m}$, as long as the mass flow rate is strictly increasing with T_s.

To further simplify the problem, we assume:

H 5. *Radiative effects are neglected.*

DOI: 10.13009/EUCASS2019-624

Using the heat equation to model the evolution of the temperature inside the solid, and the Navier-Stokes equations with reactions and species transport for the gas phase yields the equations presented without the 1D-assumption in [8]. The solid phase is represented by its temperature $T(x,t)$ and its constant density ρ_s. The gas phase is described by the density $\rho(x,t)$, the constant pressure P, the flow speed $u(x,t)$, and the temperature $T(x,t)$. The reactive aspect of the flow with n_e species (symbol $\mathcal{E}_i$) is taken into account with the addition of the transport equations for the species mass fractions $Y_i(x,t)$ and the addition of the volumetric heat release as a source term in the energy equation. The volumetric molar production rate of the i-th species is ω_i, in mol.m^{-3}.s^{-1}. We consider n_r chemical reactions of the form: $\sum_{i=1}^{n_e} \nu'_{i,r}\mathcal{E}_i \rightarrow \sum_{i=1}^{n_e} \nu''_{i,r}\mathcal{E}_i$. We introduce $\nu_{i,r} = \nu''_{i,r} - \nu'_{i,r}$, the global stoichiometric coefficient. The reaction rate of the r-th reaction is $\dot{\omega}_r$, in mol.m^{-3}.s^{-1}, and consequently $\omega_i = \sum_{r=1}^{n_r} \nu_{i,r}\dot{\omega}_r$. The molar enthalpy of the i-th species is $h_{i,mol}(T) = h^0_{i,mol} + \mathscr{M}_i c_{p,i}(T - T_{std})$ in J.mol^{-1} with $\mathscr{M}_i$ the molar mass of this species, and T_{std} the standard temperature at which all standard molar enthalpies $h^0_{i,mol}$ are defined. The enthalpies (resp. standard enthalpies) per unit mass are written h_i (resp. h^0_i). The gas and solid phases are coupled at the interface through boundary conditions obtained by integration of the energy and transport equations around the interface. Assuming the pyrolysis process is concentrated at the interface, we introduce the "injection" mass fractions Y_{i,σ^-} for the different gaseous species, which indicates the mass fractions obtained after pyrolysis directly at the interface, before entering the gas phase. Due to lack of space, we do not provide the original system, but we give the interface boundary conditions:

$$\begin{cases} T_{\sigma^-} = T_{\sigma^+} = T_s & (3) \\ -\left(\lambda_s \partial_x T\right)_{\sigma^-} = \dot{m} Q_p - \left(\lambda_g \partial_x T\right)_{\sigma^+} & (4) \\ \left(\dot{m} Y_i\right)_{\sigma^-} = \left(\dot{m} Y_i - \rho J_i\right)_{\sigma^+} \quad \forall\, i \in [\![1, n_e]\!] & (5) \end{cases}$$

Q_p is the heat of the pyrolysis reaction, per unit mass of solid propellant consumed. Equation (4) means that the heat conducted from the gas phase into the solid and the heat generated by the pyrolysis process (if the pyrolysis is exothermic) are used to heat the solid propellant and sustain the combustion. Equation (5) is the species balance, i.e. the flow rate of the i-th species generated by the pyrolysis is equal to the flow rate of this species leaving the surface in the gas phase, minus the species diffusion flow rate J_i.

We introduce the following set of additional assumptions, also shared by the classical analytical models:

H 6. *The specific heat of the solid c_s is constant. The solid phase thermal conductivity λ_s is constant.*

H 7. *The gas phase viscosity is neglected. No binary species diffusion takes place in the gas phase.*
The gas phase contains two species: the reactant G^1 and the product G^2, with mass fractions Y_1 and Y_2.
There is only one irreversible reaction $-\nu_1 G^1_{(g)} \rightarrow \nu_2 G^2_{(g)}$.
The species G^1 is completely consumed at $x = +\infty$. All gradients are zero at $x = +\infty$.
The species diffusion coefficients D_i are equal, $D_i = D_g\ \forall i$
Both species have the same molar mass $\mathscr{M}$ and therefore opposite stoichiometric coefficients ($\nu_1 = -\nu_2$).
The species specific heats c_{p_i} are all equal, $c_{p_i} = c_p\ \forall i$, with c_p the constant gas specific heat.

H 8. *The pyrolysis reaction transforms the solid propellant P into the species G^1.*

Using these assumptions, we can simplify the equations. We introduce $D_{th} = \lambda_g/(\rho c_p)$ the thermal diffusivity of the gas, and $D_s = \lambda_s/(\rho_s c_s)$ the thermal diffusivity of the solid propellant. Having only two species, we replace the transport equation for Y_2 by the global mass balance. We introduce $Q_{mol} = \mathscr{M}\left(\nu_1 h^0_1 + \nu_2 h^0_2\right)$, the molar heat of the reaction in the gas phase.

As we aim at studying steady, self-similar combustion waves, we look for a solution in the form of a travelling wave $f(x,t) = \hat{f}(x - ct)$ for all the variables. This is equivalent to performing the variable change $\hat{x} = x - ct$, as described in [13]. The speed c corresponds to the regression speed of the propellant surface, it should thus be considered negative in our study. We suppose that the interface is at the abscissa 0 in the new reference frame. In this frame, the travelling wave is a stationary solution. To highlight the fact that the variables associated with these new equations are different from the previous ones, we use the notation " $\hat{}$ ", and we introduce $\hat{Y} = \hat{Y}_1$ for the sake of simplicity. Overall, we obtain the following system of equations:

DOI: 10.13009/EUCASS2019-624

System 1.

$$\left\{ -c d_{\hat{x}}\hat{T} - D_s d_{\hat{x}\hat{x}}\hat{T} = 0 \right. \tag{6}$$

$$\begin{cases} -c d_{\hat{x}}\hat{\rho} + d_{\hat{x}}(\hat{\rho}\hat{u}) = 0 & (7) \\ \hat{\rho}(\hat{u}-c) d_{\hat{x}}\hat{Y} - d_{\hat{x}}\left(\hat{\rho} D_g d_{\hat{x}}\hat{Y}\right) = \mathscr{M}_1 \nu_1 \dot{\omega} & (8) \\ \hat{\rho}(\hat{u}-c) d_{\hat{x}}\hat{T} - d_{\hat{x}}\left(\hat{\rho} D_{th} d_{\hat{x}}\hat{T}\right) = \dfrac{\dot{\omega} Q_{mol}}{c_p} & (9) \\ \hat{\rho} = \dfrac{P\mathscr{M}}{R\hat{T}} & (10) \end{cases}$$

$$\begin{cases} \hat{T}(-\infty) = \hat{T}_0 & (11) \\ \hat{T}(0^-) = \hat{T}(0^+) = T_s & (12) \\ -\left(\lambda_s d_{\hat{x}}\hat{T}\right)_{0^-} = \dot{m} Q_p - \left(\lambda_g d_{\hat{x}}\hat{T}\right)_{0^+} & (13) \\ \left(\dot{m}\hat{Y}\right)_{0^-} = \left(\dot{m}\hat{Y} - \hat{\rho} D_g d_x \hat{Y}\right)_{0^+} & (14) \\ \partial_{\hat{x}}\hat{T}(+\infty) = 0 & (15) \\ \partial_{\hat{x}}\hat{Y}(+\infty) = 0 & (16) \end{cases}$$

The regression speed c appears in these equations in various manners: in the convective terms, in the interface boundary conditions, in the mass flow rate at the interface $\dot{m} = -\rho_s c$, and through T_s, as the mass flow rate is linked to surface temperature through (2).

2.2 Mass, species and energy balances

With the aim of performing a theoretical analysis on the previous system, we would benefit from having a dimensionless system. To do so, we first derive some balance equations based on the previous equations, in order to obtain characteristic scales from which we can build dimensionless variables. In order to avoid a notation overload, we drop the symbol " $\hat{}$ ". For further simplifications, we also introduce the following assumptions:

H 9. *The specific heats of the solid and gas phases are equal: $c_p = c_s$.*

H 10. *The Lewis number D_{th}/D_g is 1 in the gas phase, i.e. the heat and species diffusions are equivalent. We introduce $D = D_g = D_{th}$.*

Even if questionable, the assumption H9 is often used in the literature ([8, 14, 12, 15]) and the results obtained are still quantitatively correct. The main effect of this assumption is that Q_p is a constant which only depends on the standard enthalpies. Assumption H10 does not mean that D is constant. It will vary throughout the gas phase due to the density changes. Integrating the continuity, transport and energy equations in the gas phase, the heat equation in the solid phase, and using the interface boundary conditions, we can obtain obtain global balance equations. We can also introduce a dimensionless enthalpy which can be shown to be a constant in the gas phase. No proofs are given, as these properties are common and are already demonstrated in the work of Zeldovich on laminar flames [9]. We introduce $Q = -Q_{mol}/(\nu_1 \mathscr{M})$ the heat of reaction in the gas phase per unit mass of $G^1_{(g)}$ consumed.

Proposition 1. *The conservation of the mass flow rate implies: $\rho(x)\ (\ u(x) - c\ ) = -\rho_s c = \dot{m}$ for $x > 0$ The complete consumption of G^1 implies: $\int_0^{+\infty} \dot{\omega}(T(x), Y(x))dx = -\dot{m}/(\mathscr{M}\nu_1)$ The burnt gas temperature at $x = +\infty$ is $T_f = T_0 + (Q + Q_p)/c_p$.*

Under assumption H10, we can define a dimensionless combustion enthalpy which is constant in the gas phase:

$$h = -\frac{Y}{\nu_1} + \frac{\mathscr{M}_1 c_p (T - T_0)}{Q_{mol}} = \frac{\mathscr{M}_1 c_p (T_f - T_0)}{Q_{mol}}$$

Remark 1. *The complete pyrolysis reaction $P_{(s)} \rightarrow G^1_{(g)}$ can be decomposed into two successive reactions:*

- *$P_{(s)} \rightarrow G^1_{(s)}$, the transformation of the solid propellant $P_{(s)}$ into the pyrolysis product at solid state $G^1_{(s)}$, with the heat of reaction $Q_s = h^0_{P_{(s)}} - h^0_{G^1_{(s)}}$*
- *$G^1_{(s)} \rightarrow G^1_{(g)}$, the sublimation of the solid pyrolysis product $G^1_{(s)}$ into $G^1_{(g)}$, at constant temperature T_s, with the latent heat $L_v = h_{G^1_{(g)}}(T_s) - h_{G^1_{(s)}}(T_s) = (h^0_{G^1_{(g)}} - h^0_{G^1_{(s)}}) + (c_p - c_{P_{G^1_{(s)}}})(T_s - T_{std})$ with $c_{P_{G^1_{(s)}}}$ the specific heat of the pyrolysis product G^1 at solid state, which we will assume equal to the solid propellant specific heat c_s.*

This leads to $Q_p = Q_s - L_v$. Q_p is the combination of a constant heat of reaction Q_s and a latent heat of sublimation L_v that depends linearly on the surface temperature. On the opposite, the heat of reaction Q for $G^1_{(g)} \rightarrow G^2_{(g)}$ in the gas phase does not depend on temperature as both species have the same specific heat.

The assumption $c_s = c_p$ makes the upcoming theoretical analysis much easier. However, the numerical method presented further in this paper does not require this assumption.

DOI: 10.13009/EUCASS2019-624

2.3 Dimensionless equations

Using the equations from the System 1 and the results obtained in the previous part, we can now write dimensionless equations for our problem.

System 2. *Introducing* $\tilde{x} = \dfrac{x}{L}$, $\tilde{c} = \dfrac{cL}{D_s}$, $\tilde{u} = \dfrac{uL}{D_s}$, $\tilde{\theta} = \dfrac{T(\tilde{x}) - T_0}{T_f - T_0}$, $\eta = \dfrac{\lambda_s}{\lambda_g}$, *and using the notation* $\cdot' = d_{\tilde{x}}\cdot$, *we have:*

$$\begin{cases} \tilde{c}\tilde{\theta}' + \tilde{\theta}'' = 0 & \text{for } \tilde{x} < 0 \quad (17) \\ \eta\tilde{c}\tilde{\theta}' + \tilde{\theta}'' = -\Psi & \text{for } \tilde{x} > 0 \quad (18) \end{cases}$$

$$\begin{cases} \tilde{\theta}(-\infty) = 0 & (20) \\ \tilde{\theta}(0^-) = \tilde{\theta}(0^+) = \tilde{\theta}_s & (21) \\ \tilde{\theta}'(0^+) - \eta\tilde{\theta}'(0^-) = \tilde{S}(\tilde{c}) & (22) \\ \tilde{\theta}(+\infty) = 1 & (23) \end{cases}$$

$$\begin{cases} \tilde{\theta}'(-\infty) = 0 & (24) \\ \tilde{\theta}'(+\infty) = 0 & (25) \end{cases}$$

with the dimensionless heat source term:

$$\Psi(\tilde{\theta}) = \frac{L^2 Q_{mol}}{\lambda_s(T_f - T_0)}\dot{\omega}(\tilde{\theta}) \geq 0 \qquad (19)$$

with the target interface balance:

$$S(\tilde{c}) = \eta\frac{Q_p}{Q_p + Q}\tilde{c} \qquad (26)$$

In order to obtain this system for the solid phase, we take equation (6), divide it by $(T_f - T_0)$ to let θ appear, and switch the spatial derivatives from x to $\tilde{x}$ ($Ld_x = d_{\tilde{x}}$); we then multiply it by L^2/D_s to obtain (17). For the gas phase, Proposition 1 allows us to build a bijection between T and Y. Therefore everything can be expressed as a function of T, in particular the reaction rate $\dot{\omega}(T, Y)$ can then be expressed as $\tilde{\dot{\omega}}(\tilde{\theta})$. Equation (18) is obtained from (9) in a similar fashion as for the solid phase. Equation (22) can be obtained after the same kind of process, with: $\tilde{S}(\tilde{c}) = cL\rho_s Q_p/(\lambda_g(T_f - T_0)) = \tilde{c}\rho_s D_s Q_p/(\lambda_g(T_f - T_0))$. Using the global energy balance and the definitions of η, D_s, we get (22) and (26). All the other boundary conditions are direct translations of the ones from System 1.

Remark 2. *For a given value of c,* θ_s *is given by* (2)*. Therefore the second order ODE* (17) *with boundary conditions* (20) *and* (21) *has a unique solution. The same goes for the ODE* (18) *with boundary conditions* (21) *and* (23)*. Boundary conditions* (24) *and* (25) *are required for a consistent mathematical behaviour at infinity. The difficulty arises from the dimensionless interface thermal balance* (22)*. For a random value of c, it is likely that it will not be satisfied. However the dependence of this condition on c through the target interface balance S allows us to envision that some specific values of c might lead to this condition being verified (hence the name "target" for S). Therefore, the regression speed c is a key variable and can be considered as an "eigenvalue" of the problem.*

Remark 3. Ψ *has the same behaviour as the reaction rate* $\dot{\omega}$*. It is positive for* $\tilde{\theta} \in [0, 1]$ *and vanishes for* $\tilde{\theta} = 1$*, since all the fuel is burned, i.e.* $\Psi(1) = 0$*.*

Remark 4. *The sign of the temperature gradient jump across the interface* $[d_x T]_{0^-}^{0^+}$*, or equivalently* $\left[d_{\tilde{x}}\tilde{\theta}\right]_{0^-}^{0^+}$*, depends on three factors:*

- $\eta = \lambda_s/\lambda_g$ *the ratio of the thermal conductivities in the gas and in the solid*
- Q_p *the reaction heat of the pyrolysis reaction, detailed in remark 1*
- *the value of the interface temperature, which is directly related to the regression rate*

As an example, in a configuration where $Q_p = 0$*, we have* $\tilde{S}(\tilde{c}) = 0$*. If* $\eta > 1$ *then* $d_x T(0^+) > d_x T(0^-)$*, but if* $\eta < 1$*, then* $d_x T(0^+) < d_x T(0^-)$*. Let us underline that the presence of the ratio of thermal conductivities has a strong impact on the sign of the jump.*

3. Existence and uniqueness of a travelling wave solution profile and velocity

In this section, we will use the previously established dimensionless system to prove that there exists at least one value of the regression speed c such that all boundary conditions can be satisfied and the complete travelling wave problem can be solved. We then proceed to show that there is only one such value of c. For the sake of simplicity, we drop the "$\tilde{\cdot}$" notation.

DOI: 10.13009/EUCASS2019-624

3.1 Monotonicity of the temperature profile

A first step in our proof of existence is to show that the temperature profile is strictly increasing in the gas phase.

Proposition 2. *The temperature is strictly monotonous and increasing from $-\infty$ to $+\infty$. There exists a bijection between x and θ.*

This proposition is established by considering the behaviour of the temperature in the two phases successively. **Solid phase** Let $x_0 \in]-\infty, 0[$ the position of a local extremum for θ. $\theta'(x_0) = 0$, therefore equation (17) implies $\theta''(x_0) = 0$. If we integrate this equation from $-\infty$ to x_0, we get $\theta(x_0) = 0$. Therefore no local extremum can be lower than 0. If a local maximum exists at x_0, $\theta(x_0) = 0$ therefore as $\theta(-\infty) = 0$ there exists a local minimum $x_1 < x_0$, and we must have $\theta(x_1) < 0$, which contradicts our previous finding. Therefore no local extremum exists for θ in the solid phase. As $c < 0$ implies $\theta(0) = \theta_s > 0$ (see (2)), we can conclude that θ is strictly increasing in this phase. **Gas phase** We want to prove that the temperature profile is monotonous and increasing in the gas phase. Using a *reductio ad absurdum*, let's suppose that $\exists\ x_0\ /\ \theta'(x_0) = 0$, local extremum or inflection point for θ. The energy equation then reads: $\theta''(x_0) = -\Psi(\theta(x_0)) < 0$, which means that x_0 can only be a local maximum. As x_0 is local maximum, there exist $x_1 > x_0$ such that $\theta'(x_1) = 0$ and $\theta'(x) < 0\ \forall\ x \in [x_0, x_1]$. x_1 can be $+\infty$. We obviously have $\theta(x_1) < \theta(x_0)$. Integrating equation (18) from x_0 to x_1 yields: $\eta c[\theta(x_1) - \theta(x_0)] = -\int_{x_0}^{x_1} \Psi(\theta(x))dx$. The left-hand side is strictly positive, but the right-hand side is strictly negative, therefore this is not possible. No local maximum x_0 exists. Overall, θ does not have any local extremum in the gas phase, and as $\theta(+\infty) > \theta(0^+)$, θ is monotonous and increasing in the gas phase. This proof is the consequence of a much more general principle in the study of second order elliptic equations called the maximum principle [16].

We now make use of the monotonicity of θ to switch from a spatial point of view to a phase space one. The bijection between θ and x allows for a variable change from x to θ in our equations. This leads to the phase portrait equations in the phase plane $(\theta, d_x\theta)$.

System 3. *Introducing $\gamma = \theta'$, the equations from System 2 are equivalent to the following set of first-order ODEs and boundary conditions:*

$$\begin{cases} c\gamma(\theta) + \gamma(\theta)d_\theta\gamma(\theta) = 0 & \forall\ \theta \in [0, \theta_s(c)] \quad (27) \\ \eta c\gamma(\theta) + \gamma(\theta)d_\theta\gamma(\theta) = -\Psi(\theta) & \forall\ \theta \in [\theta_s(c), 1] \quad (28) \end{cases} \qquad \begin{cases} \gamma(0) = 0 & (29) \\ \gamma(1) = 0 & (30) \\ \gamma(\theta_s^+) - \eta\gamma(\theta_s^-) = S(c) & (31) \end{cases}$$

The system is established by studying the problem in the solid, using the definition of γ in equation (17) and using $d_x\gamma = d_\theta\gamma d_x\theta = \gamma d_\theta\gamma$. We obtain (27). The same process is used for the gas phase. The boundary conditions are directly obtained from the ones of the dimensionless system.

Remark 5. *This set of equations is similar to the one obtained by Zeldovich et al. [9] for a homogeneous gaseous laminar flame. In this reference, the phase portrait of the temperature profile is also split in two parts. The first one represents the part of the profile where the temperature is lower than an artificial cut-off temperature $\theta_{ignition}$, below which the reaction rate Ψ is forced to zero. This is purely a convection-diffusion zone. This allows the "cold boundary" problem [11] to be overcome. The second part of the laminar flame phase portrait is the same as ours: the gas phase undergoes a reaction which creates a steep increase in temperature before reaching the adiabatic combustion temperature behind the combustion wave. This is a convection-diffusion-reaction zone. The two zones are joined using the continuity of the temperature profile and its gradient, as no reaction or heat accumulation takes place at the interface. In our case, the first part of the phase portrait is not associated with a cut-off of the gas phase reaction rate, but with the fact that the solid phase is inert, therefore it only heats up through heat diffusion. Our problem thus differs in two ways with the laminar flame one. First, the pyrolysis reaction is concentrated at the interface and causes a discontinuity of the temperature gradient, which depends on the wave speed value c. Secondly, the position of the interface in the phase portrait θ_s also varies with c, whereas $\theta_{ignition}$ is an arbitrary constant. We can artificially make our problem equivalent to the laminar flame's one by forcing $Q_p = 0$, $\eta = 1$, $\theta_s = \theta_{ignition}$, $D_s = D_g$ (and $c_s = c_p$ as assumed in H9).*

The rest of the study will be based on the analysis of the phase portrait of the system, i.e. the plot of γ versus θ. Such a phase portrait is represented in figure 2.

DOI: 10.13009/EUCASS2019-624

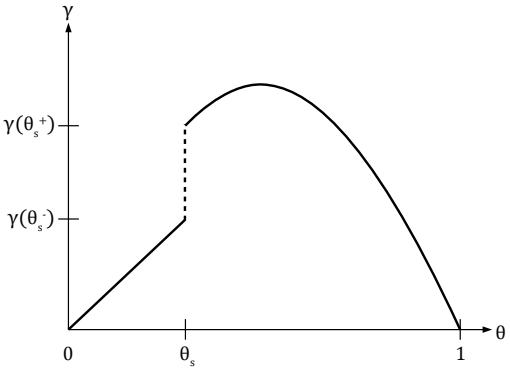

Figure 2: Schematic phase portrait in both phases

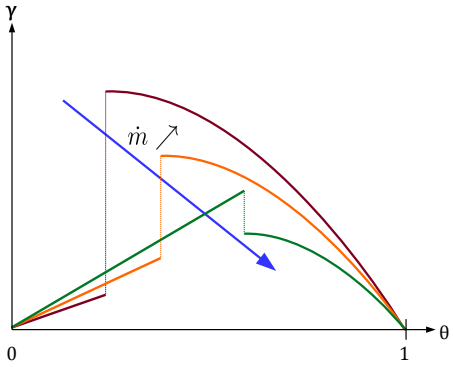

Figure 3: Evolution of the phase portrait with $\dot{m}$. Each curve corresponds to the solution curve for one value of $\dot{m}$.

3.2 Existence of a solution

We will now show that there exists at least one wave speed $c < 0$ such that the travelling wave problem previously stated has a solution. We introduce $\Delta\gamma(c) = \gamma\left[\theta_s^+(c)\right] - \eta\gamma\left[\theta_s^-(c)\right]$, the effective interface balance at wave speed c and $\xi(c) = \Delta\gamma(c) - S(c)$, which we will call the interface balance mismatch. We introduce another assumption, non-restrictive for any real application:

H 11. *The heat of the pyrolysis reaction Q_p is such that $Q_p > -Q$.*

Proposition 3. *Under the assumption H4 so that $\dot{m}(T_0) = 0$, and assuming H11, there exists at least one wave speed c such that the problem stated in System 2 can be solved. All solutions for the wave speed c reside in the interval $]\, c_{max}, 0\,[$, with c_{max} the dimensionless wave speed such that $\theta_s(c_{max}) = 1$.*

The global phase portrait in the gas and solid phases is schematically represented in figure 2. We see that both phase portraits will not join at θ_s, but rather that there will be a jump of γ at this point, as explained in remark 2. More precisely, the thermal boundary condition may be reformulated as:

$$\Delta\gamma(c) = S(c) \quad \Leftrightarrow \quad \xi(c) = 0$$

with $\Delta\gamma$ the effective interface balance, i.e. the interface balance we obtain for a given value of c by integrating equations (17) and (18) separately, and ξ the interface balance mismatch, which is non-zero when the thermal balance condition (22) is not satisfied. If the wave speed c is a good solution, then we have $\xi(c) = 0$.

To prove the existence of a value of c such that the complete travelling wave problem is solved, we have to prove that there exist at least one value of c such that this equality is satisfied. As ξ is a continuous function of c, we will try to find two values of the wave speed c_1 and c_2 such that $\xi(c_1)$ and $\xi(c_2)$ have opposite signs. That would imply that there is at least one value of $c \in [c_1, c_2]$ such that $\xi(c) = 0$. Therefore we exhibit two limit cases for the wave speed c which naturally yield a different sign for ξ:

- **Case** $c = 0$: In this case $\dot{m} = 0$, i.e. the solid propellant remains inert. Using assumption H4, we obtain $\theta_s = 0$ and we are still satisfying the monotonicity of θ shown in Proposition 2 (the monotonicity is strict only if $\theta_s > 0$). With $c = 0$, Proposition 1 yields $u = 0$. If we denote with a "0" subscript the values obtained with $c = 0$, the following equalities are satisfied $\gamma_0(\theta_s^-) = 0$, $\gamma_0(\theta_s^+) = (2\int_0^1 \Psi(y)dy)^{1/2} = (2I_0)^{1/2}$, $S(c{=}0) = 0$. Consequently $\Delta\gamma(c{=}0) = (2I_0)^{1/2} > S(c{=}0)$, and therefore $\xi(c = 0) > 0$.
- **Case** $c = c_{max}$: The solution we are looking for is monotonous and thus requires that $\theta_s < 1$.Based on the pyrolysis law, the case $\theta_s = 1$ corresponds to a certain value $c_{max} < 0$ of the wave speed. We can then directly integrate the phase portrait equations (27) and (28) and get $\gamma_0(\theta_s^-) = -c_{max}$, $\gamma_0(\theta_s^+) = 0$ and $S(c) = \eta\, c_{max}\, Q_p/(Q_p + Q)$. Thus, $\xi(c_{max}) = \Delta\gamma(c_{max}) - S(c_{max}) = \eta c_{max}\left(1 - Q_p/(Q_p + Q)\right) = \eta\, c_{max}\, Q/(Q_p + Q)$. Assuming H11, we obtain $\xi(c_{max}) < 0$.

In realistic cases for Q_p, we have shown that $\xi(0) > 0$ and $\xi(c_{max}) < 0$. Therefore, as ξ is continuous, there exists at least one value of $c \in]c_{max}, 0[$ such that $\xi(c) = 0$. This proves that there exist a solution to the problem

DOI: 10.13009/EUCASS2019-624

stated in System 3, therefore also for the dimensionless problem from System 2 and for the simplified travelling wave problem from System 1. Potential solutions with $c > 0$ or $c < c_{max}$ are physically meaningless and are not further considered.

3.3 Uniqueness of the solution

Having proved that there exists at least one value of c such that the travelling wave problem can be solved, we now proceed to show that there is only one such value. There are two cases, depending on the sign of Q_p.

Proposition 4. *If $Q_p < 0$, there exists a unique value of the wave speed c such that the travelling wave problem exposed in System 2 has a solution.*

Studying the existence of a solution, we have introduced $\xi(c) = \Delta\gamma(c) - S(c)$ the interface balance mismatch, and showed that it undergoes a change of sign between $c = 0$ and $c = c_{max}$. We now proceed to show that ξ is strictly monotonous on this interval.

In the solid phase, we have $\gamma(\theta_s(c)^-) = -c\theta_s(c)$. Deriving with respect to c, we obtain:

$$d_c\gamma(\theta_s(c)^-) = -\theta_s(c) - cd_c\theta_s(c)$$

Based on the pyrolysis law (2) and as c and $\dot{m}$ are of opposite signs, we see that $d_c\theta_s < 0$, therefore $d_c\gamma(\theta_s(c)^-) < 0$. In the gas phase, we can derive equation (18) with respect to c: $\partial_c(\partial_\theta\gamma) = -\eta + (\partial_c\gamma/\gamma^2)\Psi(\theta)$. Introducing $y = -\gamma/\eta$ and $\Pi(\theta) = \Psi(\theta)/\eta^2$, it yields $\partial_c(\partial_\theta y) = 1 + (\partial_c y/y^2)\Pi(\theta)$. Let $\mathcal{X} = \int \Pi/y^2$, the equation then has the solution ([9], page 256): $\partial_c y = -\exp(\mathcal{X})\int_z^1 \exp(-\mathcal{X})dz < 0$. Therefore, we obtain $\partial_c\gamma(\theta_s^+) = -\eta\partial_c y > 0$. Overall $\partial_c\Delta\gamma > 0$. Deriving equation (26), we get: $\partial_c S = \eta Q_p/(Q_p + Q)$. We know that Q_p is in magnitude lower than Q, therefore $\partial_c S$ has the same sign as Q_p. If $Q_p \in]-Q, 0]$, $\partial_c S < 0$, therefore we have $\partial_c\xi > 0$. As $\xi(c_{max}) < 0$ and $\xi(0) > 0$, this implies the uniqueness of the solution wave speed c.

Proposition 5. *If $Q_p > 0$, there exists a unique value of the wave speed c such that the problem stated in System 2 has a solution c, which belongs to the interval $]c_{max}, c_{min}[$ with c_{min} such that $\theta_s(c_{min}) = Q_p/(Q + Q_p)$.*

This result is obtained in a manner almost identical to the previous one. The difference lies in the behaviour of S. With $Q_p > 0$, we have $\partial_c S > 0$, as is $\partial_c\Delta\gamma$, therefore we cannot directly conclude on the sign of $\partial_c\xi > 0$ for $c \in [c_{max}, 0]$. Therefore we will now try to show that there exists a smaller interval $[c_{max}, c_{min}]$ such that $\xi(c_{min}) > 0$ and $\xi(c_{max}) < 0$, and such that ξ is strictly monotonous. This would prove that the solution is unique within this interval.

Let us introduce $k = Q/Q_p$. We can write $\partial_c S = \eta/(1 + k)$. We will now define a wave speed $c_{min}(k)$ such that there is a unique value of c in $]c_{max}, c_{min}(k)[$ such that $\xi(c) = 0$. Let us find a lower bound for $d_c\xi$:

$$\frac{1}{\eta}d_c\xi = \frac{1}{\eta}\left(d_c\gamma(\theta_s^+) - \eta d_c\gamma(\theta_s^-)\right) - \frac{1}{1+k}$$

We already proved that $d_c\gamma(\theta_s^+) \geq 0$, and that $-d_c\gamma(\theta_s^-) = \theta_s + cd_c\theta_s \geq \theta_s$, therefore:

$$\frac{1}{\eta}d_c\xi \geq \theta_s - \frac{1}{1+k}$$

Consequently, to ensure $d_c\xi \geq 0$, we have the following sufficient condition:

$$\theta_s \geq \theta_{s,min} = \frac{1}{1+k} = \frac{Q_p}{Q_p + Q} = \frac{Q_p}{c_p(T_f - T_0)} \quad \Leftrightarrow \quad T_s \geq T_{s,lim} = T_0 + \frac{Q_p}{c_p}$$

Here we can give a physical interpretation of $T_{s,lim}$. It is the temperature that would be achieved at the interface without any heat feedback from the gas phase. Indeed if $d_x T(0^+) = 0$, we can integrate equation 6 from $-\infty$ to 0 and find $T_s = T_0 + Q_p/c_s$. As we assume $c_p = c_s$, we recover our expression of $T_{s,lim}$. In our case we have shown that γ is always positive in the gas phase, therefore heat is always conducted from the gas phase into the solid phase, which results in $T_s > T_{s,lim}$. That is also what we would expect from a physical point of view, as we know the gas phase will actually heat up the solid, not cool it down.

Let us now compute $\xi(c_{min}) = \gamma(\theta^+_{s,min}, c_{min}) - \eta\gamma(\theta^-_{s,min}, c_{min}) - \eta c_{min}/(1 + k)$, that is $\xi(c_{min}) = \gamma(\theta^+_{s,min}, c_{min})$. The strict monotonicity of θ implies that γ is always positive, therefore $\xi(c_{min}) \geq 0$. As we

DOI: 10.13009/EUCASS2019-624

know that $\xi(c_{max}) < 0$, $\xi(0) > 0$ and proved that $d_c\xi(c < c_{min}) > 0$, we can conclude that there is a unique solution $c \in]c_{max}, c_{min}[$ such that $\xi(c) = 0$.

At this point, we have proved that there exists only one steady combustion travelling wave solution for the combustion of a homogeneous solid propellant with simplified kinetics and a pyrolysis concentrated at the surface. The assumption H9 ($c_s = c_p$) made the proof of uniqueness much easier. However it can easily be relaxed in the numerical method, as it only changes the definition of S, Q_p and T_f. It is likely that the solution may remain unique on a certain range of values for the ratio c_p/c_s. As highlighted in the first part, the simplified pyrolysis law can also be replaced by a more evolved one, like the ones from [12], as long as the mass flow rate is strictly increasing with the surface temperature.

3.4 Heteroclinic orbit and critical points

The points $x = -\infty$ and $x = +\infty$ are critical points for the System 1, i.e. all derivatives are zero. These points correspond to $(\theta = 0, \gamma = 0)$ and $(\theta = 1, \gamma = 0)$. The phase portrait of our system is a heteroclinic orbit that joins these two points. $(0, 0)$ is more difficult to analyse, as it is not an hyperbolic point, however we can easily integrate (17) and find that the solution is $\gamma = -c\theta$. The other point $(1, 0)$, in the gas phase, is a hyperbolic point, therefore the solution curve (orbit) will depart from the associated stable manifold. We can determine the slope $d_\theta\gamma(1)$ by means of a linearisation. We use the approximations $\gamma(\theta) = \alpha(\theta - 1)$ and $\Psi(\theta) = \beta(\theta - 1)$, with $\alpha = d_\theta\gamma(1)$ and $\beta = d_\theta\Psi(1)$. Following remark 3, we know that $\beta < 0$. Injecting these linearised expressions into (18), we get: $\alpha^2 + \alpha\tilde{m} + \beta = 0$. This second order equation corresponds to $\Delta = \tilde{m}^2 - 4\beta > 0$. We have two real solutions of opposite signs. As we require $\alpha = d_\theta\gamma(1) < 0$ so that our solution remains at $\gamma \geq 0$, we find:

$$\alpha = \frac{\tilde{m}}{2}\left(1 - \sqrt{1 - \frac{4\beta}{\tilde{m}^2}}\right) \tag{32}$$

This behaviour at critical points will be used in the numerical strategy based on a shooting method.

3.5 Physical interpretation and discussion

Let us remind the reader that the pyrolysis mass flow rate $\dot{m} = -\rho_s c$ is positive, whereas c is negative. We have seen that $\gamma(\theta_s(c)^+)$ diminishes as the mass flow rate in the gas phase increases, independently of the interface and solid phase. Therefore the heat feedback from the gas phase onto the solid diminishes as well. $\Delta\gamma(c)$ is the dimensionless thermal power excess that is available to power the pyrolysis process, i.e gas heat feedback minus the thermal power used to heat up the solid. We have $d_c\Delta\gamma > 0$, i.e. $\Delta\gamma$ diminishes as $\dot{m}$ increases, therefore increasing $\dot{m}$ (i.e. lowering c) will decrease thermal power available for the pyrolysis. $S(c)$ is the dimensionless thermal power that is required for the pyrolysis process to be sustained at the given value of c. d_cS indicates how this required thermal power evolves with the pyrolysis mass flow rate $\dot{m} = -\rho_s c$.

case $\mathbf{Q_p < 0}$ In the case $Q_p < 0$, the pyrolysis process is endothermic, i.e. it absorbs heat from the gas and solid phases. This can be the case if the sublimation of $G^1_{(s)}$ into $G^1_{(g)}$ is very demanding in terms of energy, which corresponds to $L_v > Q_s$ in remark 1. We showed that $d_cS < 0$, i.e. the thermal power required by the pyrolysis increases with the mass flow rate. If, for an arbitrarily chosen value of c, we have $\Delta\gamma(c) > S(c)$, it means that the heat feedback from the gas phase is too high compared to the heat that would be absorbed by the solid phase and the pyrolysis reaction in a stationary state. The fact that $d_c\Delta\gamma > 0$ and $d_cS < 0$ shows that as we lower the mass flow rate, the thermal power excess transmitted by the gas phase to the interface increases whereas the thermal power needed for the pyrolysis decreases. Therefore we can find a value of c such that both powers cancel out.

case $\mathbf{Q_p > 0}$ The same reasoning can be applied. In this case the pyrolysis is exothermic, thus part of the heat conducted from the gas phase into the solid is used to maintain the surface temperature. We showed that $d_cS > 0$, i.e. the thermal power required by the pyrolysis decreases as the mass flow rate increases, in the sense that it is actually negative and increasing in magnitude. This is physically coherent with the fact that the pyrolysis is exothermic. We established that in the interval $]c_{max}, c_{min}[$, $d_c\xi > 0$. It shows that as we lower the mass flow rate $\dot{m}$, the thermal power excess transmitted by the gas phase to the interface will increase more rapidly than the thermal power needed for the pyrolysis. Therefore, starting from a value of $\dot{m}$ such that the heat feedback is too strong, lowering $\dot{m}$ will only worsen the interface thermal balance. We actually need to increase $\dot{m}$, up until the point where the thermal power S required by the pyrolysis catches up with the thermal power excess $\Delta\gamma$.

DOI: 10.13009/EUCASS2019-624

The gradient jump $[d_x\theta]_{0^-}^{0^+}$ is the same as $[\gamma]_{\theta_s(c)^-}^{\theta_s(c)^+}$. Using (22), we can rewrite this as $[\gamma]_{\theta_s(c)^-}^{\theta_s(c)^+} = S(c) + (\eta - 1)\gamma\left(\theta_s(c)^-\right)$. In the particular case where $\eta = 1$, i.e. both phases have the same thermal conductivity, this reduces to $S(c)$, thus the gradient jump has the sign of S. If we have $\eta \neq 1$, the sign of the gradient jump will depend on the gradient in the solid phase at the interface. For example, if $\eta > 1$, the temperature gradient jump at the interface will be positive only if $S(c) > (1-\eta)\gamma(\theta_s(c)^-)$.

This theoretical thus study brings in two aspects. First, it allows to describe a variety of physical scenarios presented in this paragraph and shows that the modelling, even if simplified, still involves sufficient physics for applications. Second, and this is the purpose of the next section, it allows for an efficient numerical resolution at arbitrary precision.

4. Numerical method and validation against CFD code

In this section, we present the numerical shooting method employed to iteratively find the correct wave speed and the temperature profile. We also present a one-dimensional CFD code developed at ONERA for the study of solid propellant combustion. Both these methods will be compared in various test cases, in terms of solution profile as well as sensitivities to the gas phase reaction activation energy. The improvement as compared to the usual analytical models will be analyzed and some parametric study will allow a characterization of the influence of the unit Lewis number assumption.

4.1 Shooting method

Determination of the phase portrait for a given c For a given value of c, we can integrate the dimensionless equations from System 3, as first-order ODEs for the variable γ as a function of θ. In the solid phase, the integration is analytical, as we directly obtain $\gamma(\theta) = -c\theta$. This gives us the value of γ for $\theta \in [0, \theta_s(c)]$. In the gas phase, equation (28) can be written as: $d_\theta\gamma = -\eta c - (\Psi/\gamma)$. We would like to integrate this equation from $\theta = 1$ to $\theta = \theta_s$. As explained in 3.4, the starting point ($\theta = 1, \gamma = 0$) is a critical point for our system, therefore starting a numerical integration from this point is impossible. To overcome this problem, we simply use the linearized solution slope α given in (32), and start the integration from $(1 - \Delta\theta, -\alpha\Delta\theta)$ instead of from the critical point. We typically use $\Delta\theta = 10^{-6}$. To maximize the accuracy, the integration of the gas phase portrait equation is performed using the Radau5 algorithm [17], featuring an adaptive step size, with very tight tolerances ($\approx 10^{-14}$). Once the profile of γ is computed, we can go back to the spatial representation using the definition $\gamma = d_x\theta$, by computing $x(\theta) = \int_{\theta_s}^{\theta} \frac{z}{\gamma(z)} dz$, so that $x(\theta_s) = 0$.

Determination of c through a dichotomy process Based on our analysis of ξ, we know that $\xi(0) > 0$ and $\xi(c_{max}) < 0$. In the case $Q_p < 0$, we start a dichotomy from the two initial points 0 and c_{max}, the latter being computed beforehand from the global energy balance and the pyrolysis law. If $Q_p > 0$, we replace the starting value 0 with c_{min}. In both cases, ξ is monotonous between the two initial points and undergoes a change of sign, therefore convergence of the dichotomy process is ensured. For each new guess of c, we integrate the phase portrait equations as explained previously, and obtain the value of $\Delta\gamma(c)$. We compare it to the value of $S(c)$ to compute $\xi(c)$. Based on the sign of $\xi(c)$, we can shrink the interval where ξ changes sign, until the changes in c between each iteration becomes small enough. We could also perform a constrained optimization on the variable c, minimizing the objective function $f(c) = [S(c) - \Delta\gamma(c)]^2$, with the constraint $c \in [c_{max}, c_{min}]$. Practically, the optimization method is quicker to find the approximate solution, but fails at determining c as precisely as the dichotomy process, even when using tight tolerances. That is why the dichotomy method will be used primarily.

Remark 6. *This method is bound to be more accurate than the analytical models discussed in the introduction, as these models basically use the same assumptions, but also assume that the activation energy of the gas phase reaction is either infinite or zero. Our method does not need this information and will better reproduce the gas flow. This comes at the cost of having to iterate on the value of c, each time integrating numerically the phase portrait equations. However, this cost will be very low, as each iteration only requires the integration of the simple ODE* (18)*. This method is consequently very useful to perform extensive parametric studies.*

The numerical shooting method contains 3 sources of error:

- Error in the estimation of $d_\theta\gamma(1)$, used to avoid the critical point in the gas phase
- Error in the numerical integration of the gas phase temperature profile.
- Convergence precision achieved by the shooting method on the value of c

Let us address the different items in this list. First, a simple parametric study on the value of $\Delta\theta$ has shown that $d_\theta\gamma$ is a constant in the neighbourhood of the critical point. Different values of $\Delta\theta$ have been tested and the converged

DOI: 10.13009/EUCASS2019-624

regression speeds are exactly identical for all $\Delta\theta$ lower than 10^{-3}. Consequently the linearisation around the critical point is a reasonable approach and the error it produces is strictly limited. The numerical integration of the gas phase with the Radau5 algorithm with very tight tolerances is close to machine-precision, as the problem is not very stiff and the step size is dynamically adapted to maximize precision. To assert this, different values of the integration tolerance were tried, ranging from 10^{-7} to 10^{-14}. The converged regression speeds were all equal within the first 8 non-zero digits. Therefore the numerical integration is fully converged and does not cause any error. Finally, the dichotomy process usually allows to converge the solution c with a relative error of the order of 10^{-10}. Overall there is no real practical limitation to the precision of this numerical shooting method.

4.2 Reference CFD code

We wish to compare our semi-analytical model with a proven CFD code in a less restrictive framework. The aim is to verify the shooting method results and validate our assumptions. The CFD tool developed at ONERA is a Fortran code based on a finite-volume approach for the one-dimensional problem. The model has also been adapted for the study of the aluminium droplet combustion, and is exposed in [18]. The molecular diffusion fluxes are approximated using a 2nd-order central difference scheme. The convective fluxes are approximated by a first-order upwind scheme, or second-order hybrid scheme weighted by the local Pechlet number. The equations are written in their steady form in the travelling combustion wave reference frame. They are discretized alongside the boundary conditions to represent a system of coupled non-linear equations. A modified Newton method is used to determine the solution, as described in [19]. The Jacobian matrix is computed numerically by perturbing the state variables. The convergence strongly depends on the initial solution. If convergence is poor, temporal evolution terms can be added to the equations to approach the steady solution through a number of transient iterations. This code also contains an automatic grid-refinement algorithm that ensures the mesh is fine enough in the regions where the gradients or the curvature are high. The refinement is performed after each successful convergence to a steady solution, until all refinement criteria are satisfied. The code can handle detailed chemistry by accessing reaction and thermodynamic data through an interface with CHEMKIN-II. Detailed molecular transport with binary species diffusion is also possible with the use of the EGlib library. However for the comparison with the numerical shooting method, these additional capabilities will not be used. This CFD code yields solutions which are subject to different sources of errors: the quality of the discretization (refinement), the tolerance for the Newton method, and the fluxes approximations.

4.3 Numerical verification and parametric studies

4.3.1 Reference case with unitary Lewis

The first test case is the combustion of a 1D-equivalent of the AP-HTPB propellant. The values for the different properties are similar to the ones presented in [8]. The activation energy for the gas-phase reaction is E_a = 58.7 kJ = 14.0 kcal, which corresponds to an activation temperature T_a = 7216 K. The pressure is set to 5 MPa. $Q_p = 1.8 \times 10^5$ J.kg^{-1}, and $Q = 3.9 \times 10^6$ J.kg^{-1}. For the CFD code, the diffusion coefficient D_g for both species is taken as a linear function of T, such that the Lewis number $Le = (\lambda_g/(\rho(T)c_p))/D_g(T)$ is 1 across the gas phase. Figure 4 shows a visual comparison of the dimensionless temperature θ and mass fraction Y profiles. Table 1 lists the values of some important results. The agreement is very good, and has been verified for several other values of the pressure P (e.g. 0.5 MPa), thus allowing us to conclude on the verification of our numerical strategy and model implementation.

	Semi-analytical	CFD
$c\ (m/s)$	9.41×10^{-3}	9.55×10^{-3}
$T_s\ (K)$	999.5	1000.5
$Y(0^+)$	0.821	0.820
$u(0^+)\ (m/s)$	0.372	0.384
$T_f\ (K)$	3541.1	3541.1

Table 1: Comparison of the main results

4.3.2 Parametric study with variable gas phase activation energy

We know that for this simplified chemical mechanism, the activation energy E_a of the gas phase reaction will be of paramount importance. Indeed, if E_a is low, the reaction will be very strong in a narrow zone just above

DOI: 10.13009/EUCASS2019-624

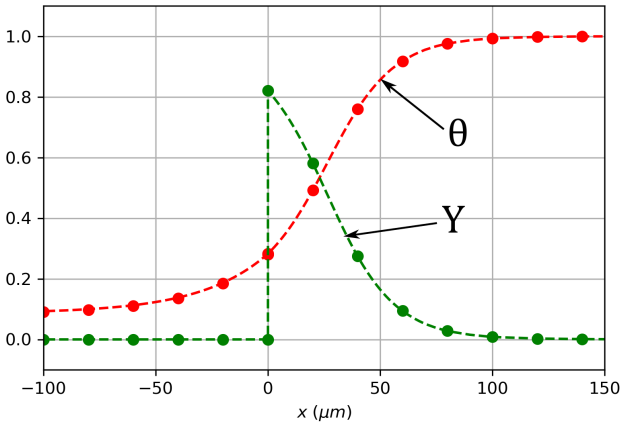

Figure 4: Plot of θ and Y of the semi-analytical solution (dots) with the numerical simulation (dashed lines)

the surface, which leads to a strong heat feedback and a high regression rate. On the opposite, if it is very large, the reaction will be spread out spatially, thus diminishing the heat feedback from the gas phase onto the solid propellant, resulting in a slower regression rate.

To highlight the effect of E_a, we compute with both methods the temperature profile for 3 values of $T_a = E_a/R$ (activation temperature), representative of low, mid and high activation energies. The pressure remains at 5 MPa. The Lewis number is 1 for both methods. All the other parameters are not modified, therefore neither the regression speed, the surface temperature, nor the gas heat feedback will be the same for all three cases.

Figure 5 shows the spatial temperature profiles. We see that as T_a decreases, the profile becomes sharper and the flame gets closer to the surface of the propellant. Figure 6 shows the phase portraits of these 3 simulations. The ordinate d_xT has been scaled for each simulation separately, so that the maximum is 1, otherwise the high values of d_xT encountered in the case $T_a = 0$ would make it difficult to see the differences. As T_a increases, we see that the abscissa T_s, i.e. the propellant surface temperature at which there is a temperature gradient discontinuity between both phases, increases and the height of the gradient jump increases. The increase of T_s is related to the increase of the heat feedback as the flame becomes thinner, which we can observe in figure 5. The evolution can be counter-intuitive at first. Indeed the gradient jump $[\gamma]_{\theta_s^-}^{\theta_s^+}$ can be linked back to the evolution of S with c. We have $Q_p > 0$, thus we know that $d_cS > 0$. Based on the pyrolysis law, we also have $d_{T_s}c < 0$ (the mass flow rate increases with T_s, therefore c becomes more and more negative). Overall we get $d_{T_s}S < 0$, and consequently $S(c) < 0$ as $S(0) = 0$. We would then expect to have a negative gradient jump with $\gamma(\theta_s^+) < \gamma(\theta_s^-)$. However we see that the opposite is true: as T_a increases, c decreases but the gradient jump increases. This is because we forgot about η which appears in the thermal interface balance condition (22). This relation tells us that if $S(c) < 0$, then $\gamma(\theta_s^+) < \eta\gamma(\theta_s^+)$. If we had $\eta = 1$, we would have a negative gradient jump. However in our case $\eta \approx 1.5$, and all the other parameters are such that we can actually obtain an increase of the gradient jump.

The fact that the gas phase portrait for $T_a = 0$ is a straight line can be surprising. This is actually related to the form of the Arrhenius law used. The reaction rate is $\dot{\omega} \propto [G^1]T\exp(-T_a/T)$. Using the constant enthalpy, expressing the concentration $[G^1]$ as $\rho Y/\mathscr{M}$ and using the ideal gas law, the linear dependence in T disappears. Switching to θ instead of T then introduces a linear dependence in $(1-\theta)$. It is then easy to verify that γ as a linear function of the form $\gamma = \alpha(1-\theta)$ is solution of equation (18).

A more thorough parametric study has been performed to obtain figure 7. The agreement of both methods for the prediction of the regression speed is very good on the whole range of activation temperatures. The relative error lies within 1.5%. An important remark is that the CFD solution very often fails to converge when the initial solution and the initial mesh are not well suited. For example, the case $T_a = 0$ involves very strong temperature gradients, which required adding many more mesh points close the surface for the initial solution. On the opposite, the case $T_a = 15000$ K gives a very smooth and slowly evolving temperature profile, but this translates to a very spread out flame, requiring additional mesh points far from the surface so that the combustion process is fully represented. Rather than remedying these problems manually, we used the semi-analytical method to generate the initial solution, and generated a mesh such that the increase in temperature between each point is not too big, and so that the mesh extends far enough from the surface so that the gas phase reaction is completed within the computational domain. This way, the CFD code converges very quickly and can further refine the mesh if needed. This highlights one of the main advantages of the semi-analytical method, which is that the solution

DOI: 10.13009/EUCASS2019-624

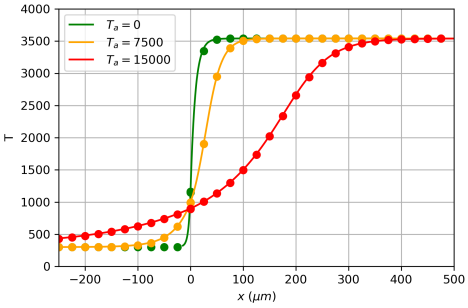

Figure 5: Temperature profiles, CFD results (full lines) compared to semi-analytical results (circles)

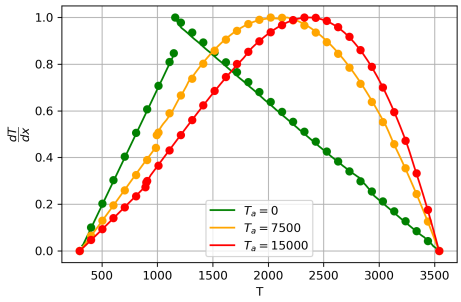

Figure 6: Normalized phase portraits, CFD results (full lines) compared to semi-analytical results (circles)

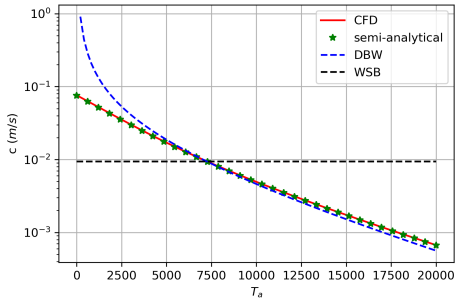

Figure 7: Regression speed as a function of activation temperature, CFD results compared to semi-analytical and analytical results

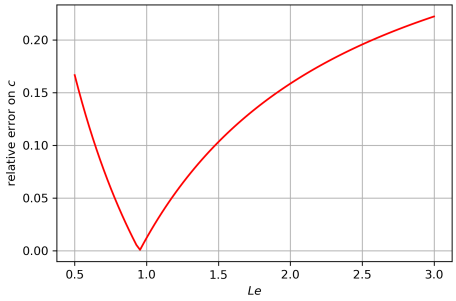

Figure 8: Relative error of c predicted by the semi-analytical method for different Lewis numbers

always converges.

Figure 7 also shows the results of the analytical models WSB and DBW. The pre-exponential factors A_p and A were adjusted so that both models predict the same regression speed at $T_a = 7216$K as the CFD model. The WSB model assumes $T_a = 0$, therefore the regression speed does not vary with T_a. We see that the tendencies are reasonable, even if not perfect agreement (we use a log scale) between the semi-analytical model and the DBW model for high activation energies. However the DBW model, which assumes high gas phase activation energy, falls apart when T_a is decreased. Overall, the semi-analytical model is a more generic model that produces quantitatively good results, without any assumption on T_a.

4.3.3 Parametric study on the Lewis number

To show the limits of the semi-analytical model, we conduct a study on the effect of a constant Lewis number, but with a value different than 1. To do so, just as before, the CFD code uses species diffusion coefficients that are linear with T, such that, as λ_g and c_p do not depend on the temperature, we have Le constant in the gas phase.

If the Lewis is high, heat diffuses much faster than species, therefore we expect steeper temperature profiles, resulting in a faster regression speed. This is confirmed in figures 9 and 10, which show the temperature profiles and phase portraits for 3 different values of Le. Figure 8 show the relative error of the semi-analytical model for the estimation of c, compared to the CFD result, for Lewis numbers within the reasonable range 0.5 to 3. As expected, the minimum error is reached around $Le = 1$. When the Lewis number is decreased below 1, the species diffuse faster than the heat, therefore the flame is more spread out. For $Le > 1$, the semi-analytical model underestimates c as it underestimates the temperature gradients around the surface. For $Le < 1$, c is overestimated. Overall, in a realistic range of Lewis numbers, the relative error lies within 20% and thus the unit Lewis number assumption still allows for a quantitatively reasonable solution.

DOI: 10.13009/EUCASS2019-624

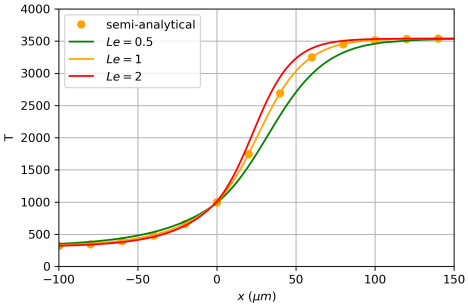

Figure 9: Temperature profiles, CFD results (full lines) compared to semi-analytical results (dots)

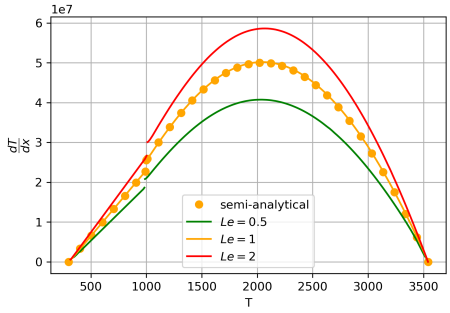

Figure 10: Phase portraits, CFD results (full lines) compared to semi-analytical results (dots)

5. Conclusion

We have presented a new method for the simplified stationary combustion of a solid propellant. The main assumptions are that the gas phase only contains one reactant and one product, the reactant being transformed into the product by a single irreversible reaction, and that the Lewis number is unitary. Considering solutions in the form of travelling waves, we have derived phase portrait equations which can be used in a numerical shooting method to determine the correct regression speed c. We have proven that the travelling wave solution profile and speed c exist and are unique under conditions which are not restrictive in view of the physical properties encountered in real solid propellants.

A numerical comparison has been conducted with a CFD code developed at ONERA, and the agreement has been found to be very good for a broad range of parameter values, at least for a unitary Lewis. We have shown that the relative error on c grows as the Lewis number Le changes, but the solution remains quantitatively good for realistic value of Le. A comparison was also made with some of the main analytical models, and we showed that semi-analytical model produced better results overall. Practically, the semi-analytical method is free of any numerical error. This method can thus be a useful verification tool for CFD codes with simplified test cases. Besides, the method always converges, hence it can be used to generate initial solutions for more detailed methods that would otherwise struggle to converge.

This method can be employed to determine the various coefficients needed to compute the linear response function to pressure fluctuations, by performing multiple simulations with slight variations of one parameter.

A few evolutions can be envisioned. More advanced pyrolysis laws can be used, as in [20]. It is also possible to consider a distributed pyrolysis, i.e. the pyrolysis process is not concentrated at the surface but spread out inside the solid. In-depth penetration of a radiative flux can also be added as a source term in the solid. Radiative fluxes entirely absorbed at the surface and radiation from the solid can be directly integrated into the presented method, by including them into the expression of S or $\Delta\gamma$. Sensitivities of the burning rate c to P and T_0 are still to be investigated. We believe that such an approach also sets the proper framework for the stability analysis of the stationary wave profile; this is out of the scope of the present paper but is the subject of our current work.

Acknowledgements

The present research was done thanks to a Ph.D grant co-funded by DGA, Ministry of Defence (E. Faucher, Technical Advisor), and ONERA.

References

[1] L. De Luca. *Theory of Nonsteady Burning and Combustion Stability of Solid Propellants by Flame Models*, chapter 14, pages 519–600. American Institute of Aeronautics and Astronautics, 1992.

[2] B. V. Novozhilov. *Theory of Nonsteady Burning and Combustion Stability of Solid Propellants by the Zeldovich-Novozhilov Method*, chapter 15, pages 601–641. American Institute of Aeronautics and Astronautics, 1992.

DOI: 10.13009/EUCASS2019-624

[3] G. Lengelle, J. Duterque, and J.F. Trubert. Physico-chemical mechanisms of solid propellant combustion. *Solid Propellant Chemistry, Combustion, and Motor Interior Ballistics*, 185:287–334, 01 2000.

[4] F. A. Williams, M. Barrere, and N. C. Huang. *Fundamental aspects of solid propellant rockets*. the Advisory Group for Aerospace Research and Development of N.A.T.O., Technivision Services; Distributed by Technical P. Slough; London, 1969.

[5] F. A. Williams. Quasi-steady gas-phase flame theory in unsteady burning of a homogeneous solid propellant. *AIAA Journal*, 11(9):1328–1330, 1973.

[6] M. W. Beckstead, R. L. Derr, and C. F. Price. A model of composite solid-propellant combustion based on multiple flames. *AIAA Journal*, 8(12):2200–2207, 1970.

[7] M.J. Ward, S.F. Son, and M.Q. Brewster. Steady deflagration of hmx with simple kinetics: A gas phase chain reaction model. *Combustion and Flame*, 114(3):556 – 568, 1998.

[8] L. Massa, T. L. Jackson, and J. Buckmaster. New kinetics for a model of heterogeneous propellant combustion. *Journal of Propulsion and Power*, 21(5):914–924, 2005.

[9] Ya.B. Zeldovich, G.I. Barenblatt, V.B. Librovich, and G.M. Makhviladze. *The Mathematical Theory of Combustion and Explosion*. Plenum Publishing, 1985.

[10] M. Verri. Asymptotic stability of traveling waves in solid-propellant combustion under thermal radiation. *Mathematical Models and Methods in Applied Sciences*, 09:1279–1305, 12 1999.

[11] H. Berestycki, B. Larrouturou, and J. M. Roquejoffre. Mathematical investigation of the cold boundary difficulty in flame propagation theory. In Paul C. Fife, Amable Liñán, and Forman Williams, editors, *Dynamical Issues in Combustion Theory*, pages 37–61, New York, NY, 1991. Springer New York.

[12] M.Q. Brewster. Combustion mechanisms and simplified-kinetics modeling of homogeneous energetic solids. *Energetic Materials: Part 2. Detonation, Combustion*, 13(8):225–294, 2003.

[13] S. Rahman. *Modélisation et simulation numérique de flammes planes instationnaires de perchlorate d'ammonium*. PhD thesis, Université Pierre et Marie Curie, 2012.

[14] T. L. Jackson and J. Buckmaster. Heterogeneous propellant combustion. *AIAA Journal*, 40(6):1122–1130, 2002.

[15] M. S. Miller. In search of an idealized model of homogeneous solid propellant combustion. *Combustion and Flame*, 46:51 – 73, 1982.

[16] H. Berestycki, L. Nirenberg, and S. R. S. Varadhan. The principal eigenvalue and maximum principle for second-order elliptic operators in general domains. *Communications on Pure and Applied Mathematics*, 47(1):47–92, 1994.

[17] E. Hairer and G. Wanner. *Solving Ordinary Differential Equations II. Stiff and Differential-Algebraic Problems*, volume 14 of *Springer Series in Comput. Math.* Springer-Verlag Berlin Heidelberg, 2nd edition, 1996.

[18] M. Muller, D. Davidenko, and V. Giovangigli. Computational study of aluminum droplet combustion in different atmospheres. In *7th European Conference for Aeronautics and Space Sciences (EUCASS)*, pages 1–17, 07 2017.

[19] M.D. Smooke and V. Giovangigli. Numerical modeling of axisymmetric laminar diffusion flames. *IMPACT of Computing in Science and Engineering*, 4(1):46 – 79, 1992.

[20] T. Jackson, L. Massa, and M.Q. Brewster. Unsteady combustion modelling of energetic solids, revisited. *Combustion Theory and Modelling*, 8:513–532, 09 2004.